Vehicle System Dynamics, 34 (2000), pp. 401–422 0042-3114/00/3406–401$15.00

Two-Degree-of-Freedom H_∞ Optimization and Scheduling for Robust Vehicle Lateral Control

SAID MAMMAR[1]

SUMMARY

In this paper, the problem of automatic vehicle steering is addressed using a two-degree-of-freedom loop shaping procedure. The controller is split into two parts. The closed loop part achieves the robust stability requirement while the prefilter part processes the reference signal and is designed to achieve model matching. The whole synthesis procedure is emphasized and the controller is tested in various situations with several system parameter variations. The observer structure of the controller is finally exploited in order to consider scheduling controllers according to vehicle speed variations. The advantages of the controller scheduling are outlined with some simulation results.

1. INTRODUCTION

Increasing the capacity of existing highways is one possible way of solving today and future transport problems. This can be achieved by intelligent highway through a more rational use of road space. However, increasing safety is also a major goal of the intelligent highway. Thus, a system capable of coordinating in a safe manner all the various operations becomes necessary. One of the basic components of this system is lateral control which permits the execution of the various positioning commands on the road.

Performing automatic steering on highway encounters significant challenges according to performance and robustness requirements. During operation, the vehicle is subject to several parameter variations and disturbances. The parameter variations are due to operation conditions (mass, speed, road-tire contact) while disturbances are due to the external forces acting on the vehicle (wind, ...).

[1]CEMIF, Université d'Évry Val d'Essonne and INRETS/LIVIC, Institut National de Recherche sur les Transports et leur Sécurité, 13 route de la Minière, 78000 Versailles cedex, France. Tel.: 33-1 40 43 29 08; Fax: 33-1 40 43 29 30; E-mail: said.mammar@inrets.fr

As a robust control method, H_∞ methodology has received many developments in its theoretical and application aspects. Globally two methods have been developed. In the first one [2] the performance and stability robustness are addressed by weighting closed loop transfer functions. The second method is due to McFarlane and Glover and is based on coprime factors system description with direct suboptimal controller solution without optimization [9]. This method also presents the advantage of converting the H_∞ robust stabilization problem into a loop shaping design procedure according to classical rules of automatic control. However, the loop shaping procedure does not directly include specifications for performance such as reference signal tracking. The two-degree-of-freedom formulation of the problem splits up simply the synthesis into robust stability achievement and robust reference model matching [4]. In this paper, this method is investigated in order to improve efficiency in the production of satisfactory controllers both for lane change and lane keeping maneuvers.

The paper is organized as follows: section 2 summarizes the two- degree-of-freedom H_∞ loop shaping procedure. The general model structure and control objectives are detailed in section 3 while controller synthesis and simulation results are carried out in sections 4 and 5. A possible way of speed scheduling of the controller is examined in section 6. It exploits the observer structure of the H_∞ controller.

2. SYNTHESIS METHODOLOGY

2.1. The Loop shaping procedure

The transfer matrix G of a $p \times m$ MIMO system can be represented using the normalized left coprime factorization: $G = \tilde{M}^{-1}\tilde{N}$, or the right coprime factorization $G = NM^{-1}$ [10]. The maximum stability margin ε_{max} is defined by the following H_∞ optimization problem over all stabilizing controllers K_∞ [15].

$$\varepsilon_{max}^{-1} = \inf_{K_\infty stabilizing} \left\| \begin{bmatrix} K_\infty \\ I \end{bmatrix} (I - GK_\infty)^{-1} \begin{bmatrix} I & G \end{bmatrix} \right\|_\infty \tag{1}$$

Let now G_i $(i = 1...N)$ be the models of the system containing the neglected dynamics in G or obtained for different parameters values of the plant. We can define for such systems a measure called the l_2-induced gap metric δ_v developed by Vinicombe [15].

Definition 1 *Consider two systems $G_1 = \tilde{M}_1^{-1}\tilde{N}_1 = N_1M_1^{-1}$ and $G_2 = \tilde{M}_2^{-1}\tilde{N}_2 = N_2M_2^{-1}$ where (N_i, M_i) are the normalized right coprime,$(\tilde{N}_i, \tilde{M}_i)$ are the normalized left coprime. The gap between G_1 and G_2 is defined as*

$$\delta_v(G_1, G_2) := \begin{cases} \| -\tilde{N}_1M_2 + \tilde{M}_1N_2 \|_\infty & \text{if the following assumption holds} \\ 1 & \text{otherwise} \end{cases}$$

The assumption is that the frequency response of $det(M_1^*M_2 + N_1^*N_2)$ does not cross the origin and its winding number is equal to zero. The winding number of a transfer

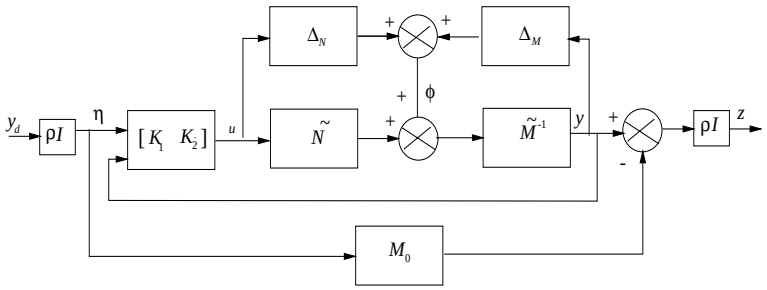

Fig. 1. Coprime factors and model matching configuration.

function G is the difference between the number of unstable poles of G^{-1} and G, assuming that G and G^{-1} are RL_∞.

There are other measures that can be used to characterize the distance between two systems, but this one gives the largest set of systems for a given ε and is easy to compute from the frequency responses [15]. The robust stabilization problem is now considered.

Theorem 2 *A controller K_∞ stabilizing the system G with a stability margin ε_{max}, will stabilize all the plants of the set $G_{\delta_v,\varepsilon} = \left\{ G_i = \tilde{M}_i^{-1}\tilde{N}_i, \delta_v(G,G_i) \leq \varepsilon \right\}$ if $\varepsilon < \varepsilon_{max}$.*

Another possible way to consider the robust stabilization problem, is to model the system uncertainties directly as additive unstructured disturbances $\left[\begin{array}{cc} \Delta_N & \Delta_M \end{array} \right]$ on the normalized coprime factors of the nominal plant G (Fig. 1). Following this representation, one can define the family of perturbed plant G_ε as follows [10]

$$G_\varepsilon = \left\{ G_p : \left[\begin{array}{cc} \Delta_N & \Delta_M \end{array} \right] \in \Re H_\infty, \left\| \left[\begin{array}{cc} \Delta_N & \Delta_M \end{array} \right] \right\|_\infty < \varepsilon \right\} \tag{2}$$

where G_p is given by (Fig. 1)

$$G_p = \left(\tilde{M} - \Delta_M \right)^{-1} \left(\tilde{N} + \Delta_N \right) \tag{3}$$

Coprime factors uncertainty may be used to model system parameter variations and neglected dynamics. The maximum stability margin $\varepsilon_{\max}$ is directly computed from equation (4)[9].

$$\varepsilon_{\max} = \left\{ 1 - \left\| \left[\begin{array}{cc} \tilde{M} & \tilde{N} \end{array} \right] \right\|_H^2 \right\}^{1/2} > 0 \tag{4}$$

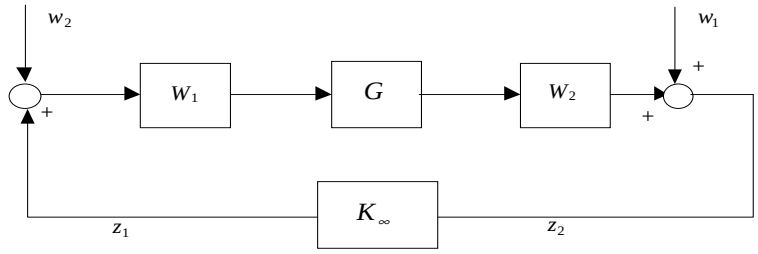

Fig. 2. Loop shape configuration.

We can note from equation (4) that the maximum stability margin depends only on the nominal system G, and not on the controller. McFarlane and Glover proposed a controller design method [9]. In this method, the performance and stability robustness trade-off are addressed using a loop shaping procedure. The closed loop design specifications are translated into constraints on the open loop transfer function. The first step of the design procedure is thus to alter the open loop singular values in order to obtain the desirable form. This is carried out using a precompensator W_1 and a post-compensator W_2 (Fig. 2). It yields to the shaped plant $G_s = W_2GW_1$. Secondly, a sub-optimal H_∞ controller K_∞ is designed, which satisfies for ε less than the stability margin of the shaped plant the following 4-bloc criterion

$$\left\| \begin{bmatrix} K_\infty \\ I \end{bmatrix} (I - G_s K_\infty)^{-1} \begin{bmatrix} I & G_s \end{bmatrix} \right\|_\infty \leq \varepsilon^{-1} \tag{5}$$

The criterion corresponds to the ∞ norm of the transfer function from disturbances w_1 and w_2 to outputs z_1 and z_2 (Fig. 2). ε is generally chosen at a value a little smaller than the stability margin. The final controller is obtained by combining K_∞ with the weights (6). When including the H_∞ controller into the loop, the open loop transfer functions GK and KG remain close to G_s [5]. The purpose of the controller is to stabilize the shaped plant G_s with minimum loop shaping degradation.

$$K = W_1 K_\infty W_2 \tag{6}$$

We can note that reference signals are not considered in the synthesis procedure. However, there are several techniques for introducing reference signals into the closed loop system. These techniques are detailed in [16], however the two-degree-of-freedom controller synthesis gives a natural manner of introducing such signals during the synthesis procedure. This is examined below.

2.2. The two-degree-of-freedom formulation

The two-degree-of-freedom configuration of a controller permits the separate processing of the reference and measurement signals. Let y_d, u, and y be respectively the reference signal, the control input and the measurement. According to the configuration of

Figure 1, the controller can be split into two parts $K_1$and K_2. The control input is then given by

$$u = K_1 y_d + K_2 y \tag{7}$$

K_1 acts as a prefilter of the reference signal while the feedback controller K_2 ensures robust stability. Suppose now that it is necessary to specify some time domain objectives such as overshot of step response and settling time. These objectives cannot be translated accurately into frequency domain specification and can therefore hardly be taken into account in the loop shape. One possible way is to group all these time domain objectives into a diagonal transfer matrix M_o, which may be considered as the desired closed loop transfer function between y_d and y (Fig. 1). The controller objectives are twofold. The first is the requirement of internal robust stability of the closed loop system. The second objective is keeping the weighted error signal z small for the entire family G_ε. This fact constitutes robust model matching. The purpose of parameter ρ is to weight the trade-off between robust stability and robust model matching. The following theorem gives a sufficient condition for a controller to satisfy both objectives.

Theorem 3 *Without loss of generality, consider that $\rho = 1$. If the following condition holds for any perturbed plant G_p of the family G_ε,*

$$\left\| \begin{bmatrix} (I - G_p K_2)^{-1} G_p K_1 - M_o & (I - G_p K_2)^{-1} \tilde{M}^{-1} \\ G_p (I - K_2 G_p)^{-1} K_1 & (I - G_p K_2)^{-1} \tilde{M}^{-1} \\ (I - K_2 G_p)^{-1} K_1 & K_2 (I - G_p K_2)^{-1} \tilde{M}^{-1} \end{bmatrix} \right\|_\infty \leq \varepsilon^{-1}$$

then the closed loop system is stable for every G_p element of G_ε, and the closed loop system achieves the following robust model matching property [4]

$$\left\| (I - G_p K_2)^{-1} G_p K_1 - M_o \right\|_\infty \leq \varepsilon^{-1}$$

In the previous theorem, the two controller components are directly computed in one step using iterative H_∞ standard optimization [3]. It is also possible to consider another robust model matching problem in which K_2 is synthesized using the non iterative method of McFarlane and Glover while the prefilter K_1 is obtained as a parameterization of controller K_2. This is summarized in the following theorem [4, 8, 17].

Theorem 4 *Given a nominal shaped plant G_s and a two-degree-of-freedom controller $K = [K_1, K_2]$,*

$$\left\| \begin{bmatrix} I \\ K_2 \end{bmatrix} (I - G_s K_2)^{-1} \begin{bmatrix} I & G_s \end{bmatrix} \right\|_\infty \leq \varepsilon_2^{-1}$$

$$\left\| \begin{bmatrix} M_0 + N Q_1 \\ M Q_1 \end{bmatrix} \right\|_\infty = \varepsilon_1^{-1}$$

$$K_1 = -(M - K_2 N)Q_1$$

where Q_1 is a stable RH_∞ transfer function, ensures that the system is stable for all perturbed plants G_p such that $\delta_v(G_s, G_p) < \varepsilon_2$ and the robust model matching performance index

$$\left\|(I - G_p K_2)^{-1} G_p K_1 - M_0\right\|_\infty \leq (\varepsilon_1^{-1} + \varepsilon_2^{-1})^{1/2}$$

is achieved for the family G_Δ generated by $G_p = G_s(1 + \Delta)$ with Δ such that G_s and G_p have the same number of unstable poles and $\|\Delta\|_\infty < \gamma^{-1}$,$\gamma \geq (\gamma_1^2 + \gamma_2^2)^{1/2}$.

In this case, robust stability in ensured in the gap metric while robust model matching is ensured for input multiplicative uncertainty. This uncertainty representation is suitable for modeling actuator bandwidth limitation and delay.

The synthesis procedure can be summarized as follows

- choose the precompensator W_1 and the postcompensator W_2 according to the classical rules of the H_∞ loop shaping procedure and form the shaped plant G_s
- compute the stability margin of the shaped plant
- compute the induced gap-metric δ_v for a mesh gridding values of the system parameter variations
- if the induced gap-metric is greater than the maximal stability margin, we must choose other precompensator and postcompensator and iterate on the previous items
- else choose the diagonal matrix function M_o according to the design time domain specification. This transfer function is usually a first or second order lag filter
- select a ρ which expresses the trade off between robust stability and robust model matching
- select a $\gamma = \varepsilon^{-1}$ a little bit greater than $1/\varepsilon_{\max}$
- compute the suboptimal H_∞ controller $K = \left[\begin{array}{cc} K_1 & K_2 \end{array}\right]$ for the standard H_∞ system interconnection given by (Fig. 3) [3, 7]

$$\left[\begin{array}{c} z \\ y \\ u \\ - \\ \eta \\ y \end{array}\right] = \left[\begin{array}{cc|c} -\rho^2 M_o & \rho\tilde{M}_s^{-1} & \rho G_s \\ 0 & \tilde{M}_s^{-1} & G_s \\ 0 & 0 & I \\ \hline \rho I & 0 & 0 \\ 0 & \tilde{M}_s^{-1} & G_s \end{array}\right] \left[\begin{array}{c} y_d \\ \phi \\ - \\ u \end{array}\right] \tag{8}$$

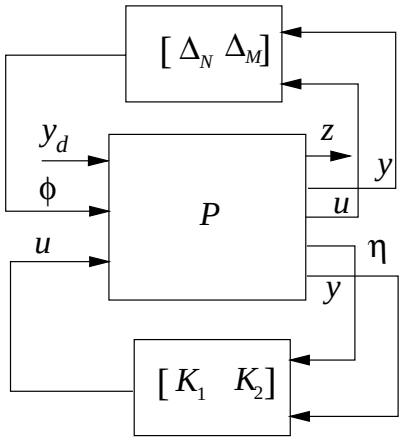

Fig. 3. Standard H_∞ problem formulation of two-degree-of-freedom controller.

where ϕ is the input from the perturbation, η is the weighted reference and $G_s = \tilde{M}_s^{-1}\tilde{N}_s$. Instead of using theorem 3, the controller can also be computed from theorem 4 in two steps using two different H_∞ optimizations.

- put the pre- and postcompensators into the feedback part K_2 according to the equation (6) and adjust the steady state gain of the prefilter so that the static gain between y_d and y will be one.

The controller synthesis procedure presented above is now applied to vehicle lateral control.

3. VEHICLE MODELING AND TASKS

A linear model of the lateral motion of the vehicle can be derived from a linearization of the non-linear kinematic equations, assuming small angles. System parameter variations, unmodeled dynamics or disturbance are considered as plant uncertainties. The well used fifth order vehicle linear lateral model is used here, it is obtained by projection of the kinematic equations on the longitudinal axis [1], (Fig. 4)

$$\begin{bmatrix} \dot{\beta} \\ \dot{r} \\ \Delta\dot{\psi} \\ \dot{y} \\ \dot{\delta}_f \end{bmatrix} = \begin{bmatrix} a_{11} & a_{12} & 0 & 0 & b_1 \\ a_{21} & a_{22} & 0 & 0 & b_2 \\ 0 & 1 & 0 & 0 & 0 \\ v & l_s & v & 0 & 0 \\ 0 & 0 & 0 & 0 & 0 \end{bmatrix} \begin{bmatrix} \beta \\ r \\ \Delta\psi \\ y \\ \delta_f \end{bmatrix} + \begin{bmatrix} 0 \\ 0 \\ 0 \\ 0 \\ 1 \end{bmatrix} u_f + \begin{bmatrix} 0 \\ 0 \\ -v \\ 0 \\ 0 \end{bmatrix} \rho_{ref} \qquad (9)$$

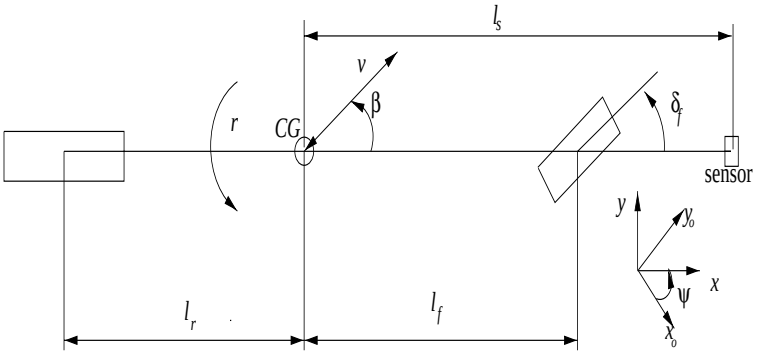

Fig. 4. Single-track model.

where

$$\begin{array}{ll} a_{11} = \frac{-(c_r+c_f)}{\tilde{m}v} & a_{12} = -1 + \frac{c_r l_r - c_f l_f}{\tilde{m}v^2} \\ a_{21} = \frac{c_r l_r - c_f l_f}{\tilde{J}} & a_{22} = -\frac{c_r l_r^2 + c_f l_f^2}{\tilde{J}v} \\ b_1 = \frac{c_f}{\tilde{m}v} & b_2 = \frac{c_f l_f}{\tilde{J}} \end{array} \tag{10}$$

$\tilde{m} = m/\mu$ is the virtual mass, $\tilde{J} = J/\mu = \tilde{m}i^2$ is the yaw moment of inertia, l_s is the distance from the vehicle center of gravity (CG) to the sensor (Fig. 4). l_r and l_f are respectively the distance from the rear and the front axle to the center of gravity. c_r and c_f are the cornering stiffness. The state vector components are the sideslip angle β, the yaw rate r, the difference between the yaw angle of the vehicle and the yaw angle imposed by the curve $\Delta\psi$, the lateral displacement y at the sensor location and the steering angle δ_f. The plant control variable will be the front steering angle rate. In the following, it will be assumed that only $\Delta\psi$ and y are measured. The trajectory to be followed is described by the road curvature ρ_{ref}. Control synthesis and simulations will be conducted for a medium class vehicle as described in [13, 14].

Three kinds of plant uncertainties have to be considered. First of all, the mass m of the vehicle varies in the range $[1330, 1573]\ Kg$. It is assumed that the common road adhesion μ varies in the range $[0.75, 1]$. So the total range of the virtual mass is $[1330, 1773]\ Kg$. Secondly, the nominal forward velocity v may be changed from $15\ m.s^{-1}$ to $40\ m.s^{-1}$. These variations significantly alter the parameter values of the state space model. The others model data are maintained constant $l_f = 1.034\ m$, $l_r = 1.491\ m$, $l_s = 1.4\ m$, $c_f = 50400\ N.rad^{-1}$, $c_r = 33600\ N.rad^{-1}$ and $J = 2783\ Kg.m^2$.

For automatic steering, the design performance objectives can be defined in terms of maximal lateral displacement from the guideline and lateral acceleration maximal boundary. The first objective is set to $3\ cm$. The second objective is set for passengers comfort, the maximal allowed value is $2\ m.s^{-2}$ $(0.2\ g)$ with a maximal overshot of

$(0.1g)$ from this value. The previous objectives are limited by two steering actuator constraints: the maximal steering angle value and rate.

Vehicle lateral control can be divided into lane change maneuver on straight road (LCM) and lane keeping maneuver (LKM). The lane change maneuver in curves can be considered as general lane change. Considering the configuration of Figure 5, the LCM can be viewed as a tracking problem with a reference signal $y_d = 3\ m$ which corresponds to the distance between the center line of two adjacent lanes. The lane change maneuver can be divided into the transition phase and the settling phase. The transition phase is defined as the phase from the initiation of the lane change command to the moment when the vehicle is within $10\ cm$ of the center of the adjacent lane. This transition phase must be as short as possible while fulfilling ride quality requirement in terms of maximal lateral acceleration and jerk. During the settling phase the lateral displacement from the center lane must be less than $5\ cm$. From the vehicle point of view, a lane keeping maneuver requires the controller to reject lateral acceleration and yaw rate disturbances caused by change in the radius of curvature. In fact, in this configuration, the reference curvature is an external input for the system (Fig. 5).

4. CONTROLLER DESIGN

Recall that lateral control of a vehicle is defined as a combination of a tracking problem, according to the lane change maneuver (LCM) and a disturbance rejection problem associated with lane keeping. The control takes then the configuration of Figure 2. In [12], a prefilter configuration is chosen in order to convert the constant relative lateral position command into the smooth relative lateral position trajectory. This configuration requires however distinct synthesis of two H_∞ controllers. The two-degree-of-freedom configuration of the controller avoids this requirement and allows a direct specification of the desired trajectory via the diagonal system matrix M_0.

The choice of pre- and postcompensators is as follows. The precompensator W_1 is chosen as a first lead filter in order to counteract the low pass integrator effect of the actuator (11). The postcompensator W_2 is chosen as a diagonal lead filters matrix (12). The filter on y enhances the speed of response by increasing the bandwidth, and increases the robustness margin by reducing the roll-off rate near the crossover frequency [6]. This effect can be seen from Figure 6 where the singular values of the transfer function from the steering angle rate to the lateral displacement are plotted for the nominal system (solid line) and the shaped one (dashed line). The filter on $\Delta\psi$ has the same effect as the one on y. The effect of these filters on the stability margins can be quantified by computing the maximal stability margin for the nominal plant and the shaped plant. This stability margin is improved by a factor 4.33. The induced gap-metric δ_v is then computed for a mesh gridding values of the speed and virtual mass variation ranges. Figure 7 shows that the ratio between the gap-metric and the maximum stability margin of the system is less than 1, this means that the controller

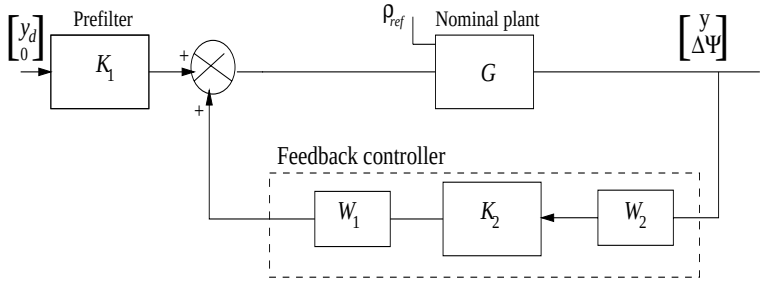

Fig. 5. Controller implementation.

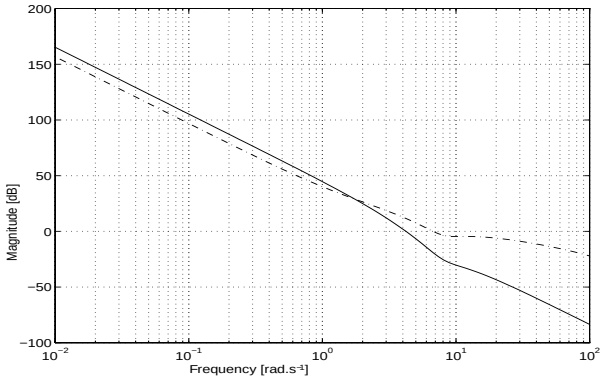

Fig. 6. Singular values shape from steering angle rate to lateral displacement.

which stabilizes the nominal system with $m = 1550\ Kg$ and $v = 25\ m.s^{-1}$ with the previous weighting filters will stabilize all the perturbed plants.

$$W_1 = \frac{s+1}{10^{-2}s+1} \tag{11}$$

$$W_2 = diag\left\{\ 0.375\frac{0.5s+1}{5\times10^{-3}s+1},\quad 0.01\frac{0.5s+1}{13\times10^{-3}s+1}\ \right\} \tag{12}$$

The time response reference model on the lateral displacement y is selected to be a second order transfer function on y and a first order on $\Delta\psi$

$$M_o = diag\left\{\ \frac{1}{s^2+2s+1},\quad \frac{1}{3.14s+1}\ \right\} \tag{13}$$

this ensures a unitary static gain and a settling time of $6\ s$. The controller is finally synthesized for the interconnection structure with $\gamma = 3.1$. The final control structure implementation then takes the form given in Figure 5.

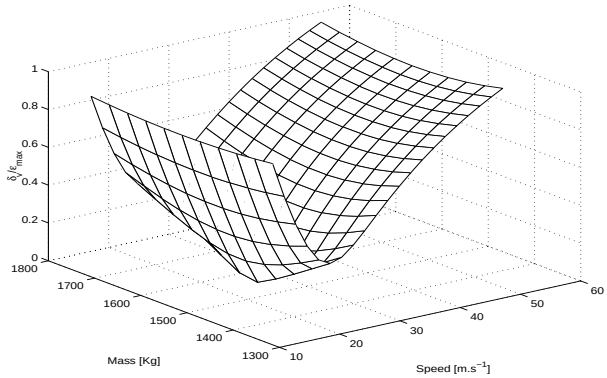

Fig. 7. Induced gap metric for mass and speed variations.

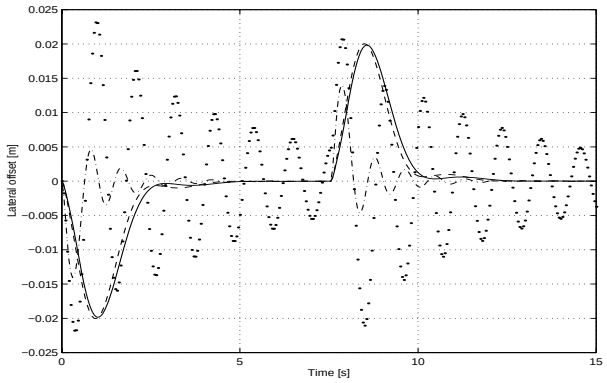

Fig. 8. Lateral offset, LKM 1.

5. SIMULATIONS

Analysis of the closed loop system behaviour is now performed for various maneuvers. The simulations are conducted on the four vertex systems

- system (S_o) (resp. (S_1)) for minimal (resp. maximal) virtual mass and minimal speed $(15\ m.s^{-1})$
- system (S_2) (resp. (S_3)) minimal (resp. maximal) virtual mass and maximal speed $(40\ m.s^{-1})$

In all of the figures, the full line corresponds to the responses of the vertex system S_o, the dashed line is for S_1, the dashdot is for S_2 and the dotted line is for S_3.

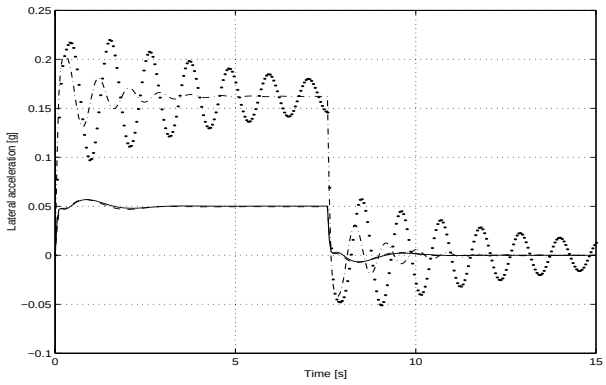

Fig. 9. Lateral acceleration, LKM 1.

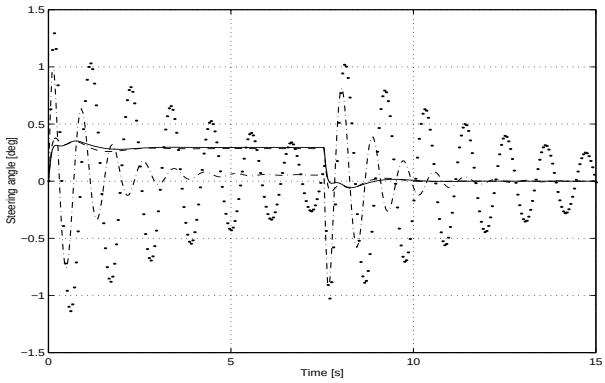

Fig. 10. Steering angle, LKM 1.

5.1. Lane keeping maneuver

In this section the controller performance is investigated on a road section where the vehicle enters a curve and exits $7.5\ s$ later to a straight road. For this maneuver, the vehicle enters a curve with a curvature $1/470\ m^{-1}$ for the minimal speed, and a curvature decreased of $1/1000\ m^{-1}$ for the maximal speed. These curvatures are the maximum allowed safety curvatures at these speeds. Figures 8 to 10 show the responses of the four vertice systems. In this case the prefilter part of the controller is not involved. One can see that the lateral offset is less than $2.5\ cm$ during the transition phase and is near zero in the steady state. The lateral acceleration and the steering angle design constraints are fulfilled. When the speed increases the overshot from the guideline increases and the responses oscillate but still remain within the prescribed limits.

Figure 11 and 12 show the results obtained for the following maneuver: at a speed

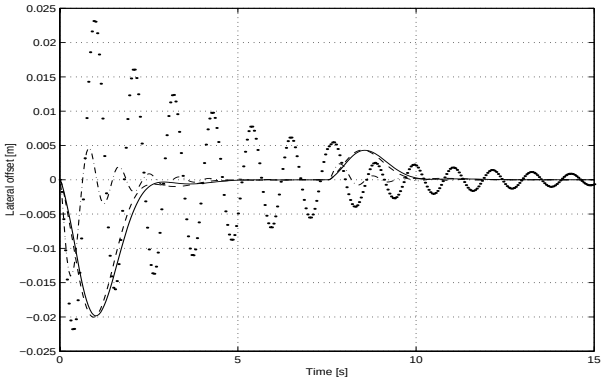

Fig. 11. Lateral offset, LKM 2.

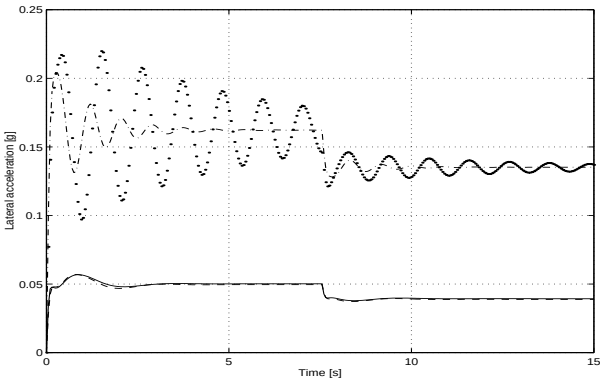

Fig. 12. Lateral acceleration, LKM 2.

of $15\ m.s^{-1}$, the vehicle enters a curve of $1/470\ m^{-1}$ and exits $7.5\ s$ later to a curve of $1/600\ m^{-1}$. At a speed of $40\ m.s^{-1}$, the vehicle enters a curve of $1/1000\ m^{-1}$ and exits $7.5\ s$ later to a curve of $1/1200\ m^{-1}$. The outputs for the first phase are the same as those obtained for the previous maneuver, but the overshot from the steady state at $7.5\ s$ is smaller because the gradient in the road curvature is smaller.

5.2. Reaction to wind gust

Wind gust forces can be considered as extra input f_w to the system acting at a distance l_w from the center of gravity (CG). The state space equation (9) must be updated with the two following equations

$$\begin{cases} \dot{\beta} = a_{11}\beta + a_{12}r + b_1 u_f + \frac{1}{mv}.f_w \\ \dot{r} = a_{21}\beta + a_{22}r + b_2 u_f + \frac{l_w}{J}.f_w \end{cases} \tag{14}$$

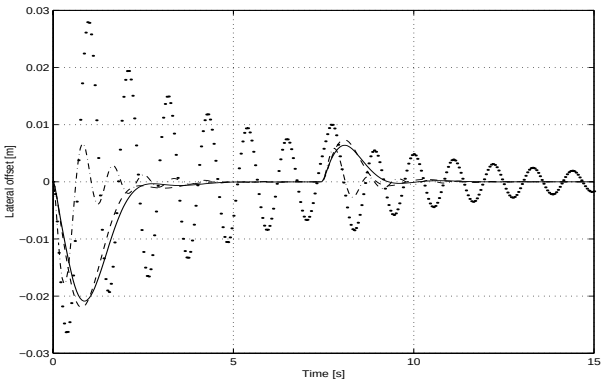

Fig. 13. Lateral offset, LKM2 and wind gust.

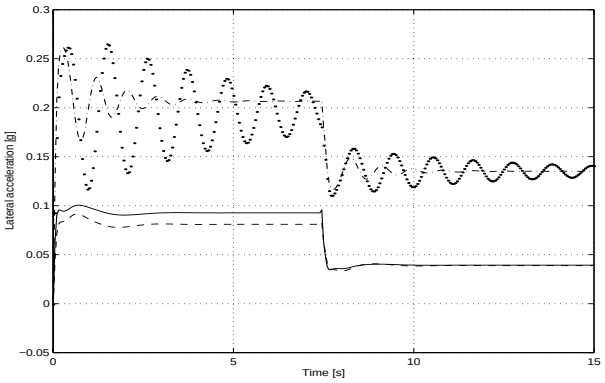

Fig. 14. Lateral acceleration, LKM and wind gust.

The vehicle is now assumed to move on the previous curve and is subject to a wind gust of $600\ N$ acting at $0.1\ m$ from the center of gravity. It is also assumed that the wind gust suddenly disappears when the vehicle enters the second curve at $7.5\ s$. The comparison of Figures 11 and 13 shows that the lateral displacement is not significantly affected by this disturbance. It is less than 3 cm. It appears from Figure 14 that the overshot of the lateral acceleration from its steady state value is within the limit of $0.1\ g$.

5.3. Lane change maneuver

The synthesized control is now tested in the case of a lane change maneuver. The lane change maneuver is considered first on a straight road, and then on a curved road. The curved road is the one considered in the second lane keeping maneuver. One can see from Figures 15 and 18 that the lateral displacement response is very close to the

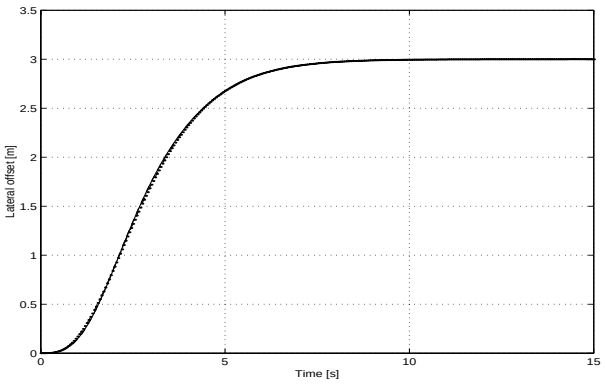

Fig. 15. Lateral offset, LCM on straight road.

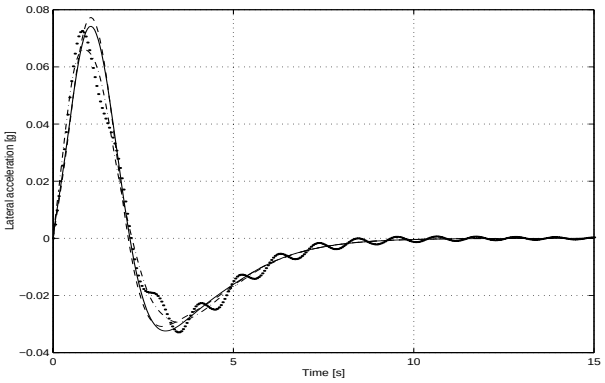

Fig. 16. Lateral acceleration, LCM on straight road.

specified model response M_o for all vertice systems. Limits on both lateral acceleration and actuator constraints are fulfilled in Figures 16, 17 and 19.

In the next section, the controller scheduling according to speed variations is considered. The aim is the reduction of response oscillations observed for the high values of speed and virtual mass.

6. CONTROLLER SPEED SCHEDULING

The forward speed of the vehicle is chosen here to the measured parameter which will be used for controller selection. The observer structure of the loop shaping H_∞ controller can be used to realize a simple controller scheduling procedure. In fact the controller resulting from loop shaping approach can be written as an exact plant

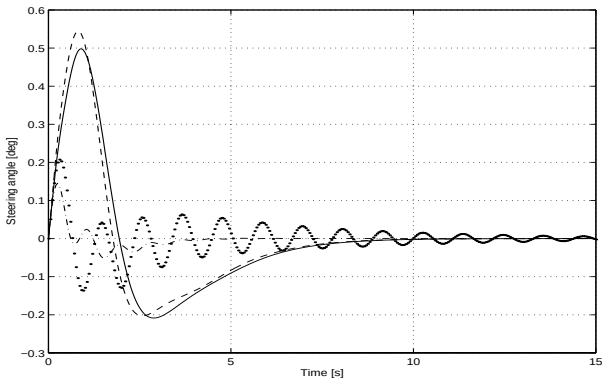

Fig. 17. Steering angle, LCM on straight road.

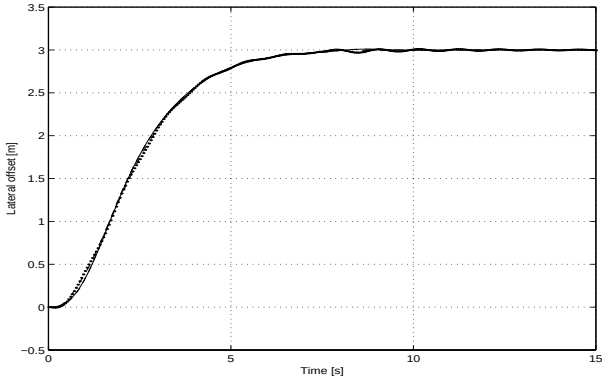

Fig. 18. Lateral offset, Lane change on curved road.

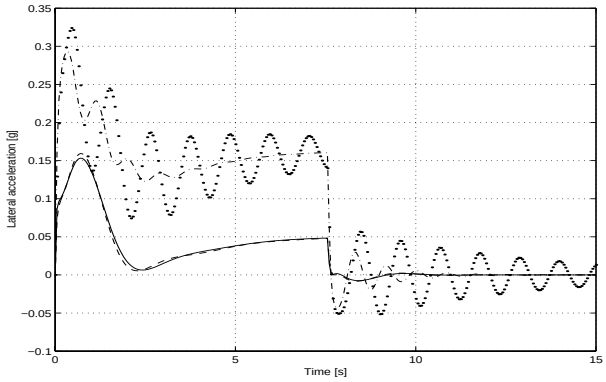

Fig. 19. Lateral acceleration, Lane change on curved road.

observer plus state feedback

$$\begin{cases} \dot{\hat{x}} = A_s\hat{x} + H(C_s\hat{x} - y) + B_s u \\ u = F\hat{x} \end{cases} \tag{15}$$

where A_s, B_s, C_s are the state space matrices of the shaped plant G_s, $H = -ZC_s^T$, and $F = B_s'(\varepsilon^2 I + \varepsilon^2 XZ - I)^{-1}X$ where X and Z are the associated control and filtering algebraic Riccati equations solutions [10]. As the system state space matrices vary smoothly with speed change, it is possible to make H and F scheduled as a function of the forward speed v. For example, The matrices between two adjacent speeds v_i and v_{i+1} are obtained by

$$\begin{cases} F(v) = (1-\alpha)F_i + \alpha F_{i+1} \\ H(v) = (1-\alpha)H_i + \alpha H_{i+1} \end{cases} \tag{16}$$

where α is a positive number between 0 and 1. However the stability of the system for v between v_i and v_{i+1} is not ensured. The following theorem gives a sufficient condition using a set of linear matrix inequalities and positive definite matrices L_i and P_i.

Theorem 5 *[18] Consider a set of controllers K_2^i $(i = 1, ..., q)$ such that each element is synthesized for a particular speed $(A(v_i), B(v_i))$ $(v_{\min} = v_1 < v_2 < ... < v_q = v_{\max})$. These controllers may be decomposed in state feedback and observer matrices (F_i, H_i). Suppose now that there exists a set of positive definite matrices L_i et P_i and a positive scalar γ such that*

$$L_i \left(A(v) + B(v)F_i\right)^T + \left(A(v) + B(v)F_i\right) L_i \leq -\gamma I$$

and

$$\left(A(v) + H_i C\right)^T P_i + P_i \left(A(v) + H_i C\right) \leq -\gamma I$$

for $v \in [a_i, b_i]$, $[a_i, b_i] \cap [a_{i+1}, b_{i+1}] \neq \emptyset$ and $\cup [a_i, b_i] = [v_{\min}, v_{\max}]$, then the scheduled controller $K_2(v) = (F(v), H(v))$ with

$$F(v) = \begin{cases} F_i & v \in [v_i, c_i[\\ \left(\frac{d_i - v}{d_i - c_i} F_i L_i + \frac{v - c_i}{d_i - c_i} F_{i+1} L_{i+1} \right) L^{-1}(v) & v \in [c_i, d_i] \\ F_{i+1} & v \in]d_i, v_{i+1}] \end{cases}$$

$$H(v) = \begin{cases} H_i & v \in [v_i, c_i[\\ P^{-1}(v) \left(\frac{d_i - v}{d_i - c_i} P_i H_i + \frac{v - c_i}{d_i - c_i} P_{i+1} H_{i+1} \right) & v \in [c_i, d_i] \\ H_{i+1} & v \in]d_i, v_{i+1}] \end{cases}$$

and

$$\begin{cases} L(v) = \left(\frac{d_i - v}{d_i - c_i} L_i + \frac{v - c_i}{d_i - c_i} L_{i+1} \right) & v \in [c_i, d_i] \\ P(v) = \left(\frac{d_i - v}{d_i - c_i} P_i + \frac{v - c_i}{d_i - c_i} P_{i+1} \right) & v \in [c_i, d_i] \end{cases}$$

where c_i and d_i are chosen such that

$$[c_i, d_i] \subset [a_i, b_i] \cap [a_{i+1}, b_{i+1}]$$

exponentially stabilizes the system $(A(v), B(v))$ for all speeds v in the range $[v_{\min}, v_{\max}]$ and verifying

$$|\dot{v}(t)| < \min_{i=1,\ldots,q-1} \left\{ \frac{d_i - c_i}{\max\{\|L_{i+1} - L_i\|, \|P_{i+1} - P_i\|\}} \right\}$$

6.1. Scheduled controllers design

First the speed range from $20\ m.s^{-1}$ to $40\ m.s^{-1}$ is sampled by covering it with a mesh consisting of 5 equally spaced grid points denoted v_i. The controller design is reconsidered, firstly we make use of two parameters k_1, and k_2.

$$W_1 = k_1 \frac{s+1}{10^{-2}s+1} \tag{17}$$

$$W_2 = diag\left\{ \ k_2 \tfrac{0.5s+1}{5\times10^{-3}s+1}, \quad 0.01 \tfrac{0.5s+1}{13\times10^{-3}s+1} \ \right\} \tag{18}$$

For each grid point v_i, the two parameters are chosen in order to maximize the stability margin. The stability margins and the associated parameters are given in table 1.

Table 1 shows that the maximum achievable stability margin is almost the same for all the speeds. A controller is finally synthesized for each of speed operating point for a relaxed value ϵ of ϵ_{max} using the procedure developed above. Scheduling matrices L_i and P_i are obtained afterwards from LMI constraints of theorem 5 using the LMI solver of [3]. The implementation configuration of the scheduled controllers is shown on Figure 20. Simulation results are detailed in the next section.

6.2. Evaluation of the scheduled controllers

The scheduled controller is tested in the case of lane keeping maneuver on the road curvature profile shown on Figure 21. In order to capture the advantages of speed scheduling, simulations are conducted in two different ways: speed varying with fixed controller and speed varying with scheduled controllers. In the figures, the solid lines correspond to the fixed controller simulation while dashed ones to the scheduled ones. The speed variations considered here are between $40\ m.s^{-1}$ and $20\ m.s^{-1}$. The speed is assumed to be uniformly decreasing during simulation from its maximum value to its minimum value. Figures 22 to 25 show that the lane keeping maneuver, with the scheduled controllers, is performed in better conditions. The lateral acceleration is attenuated while all other responses present smaller maximum offset and are less oscillatory.

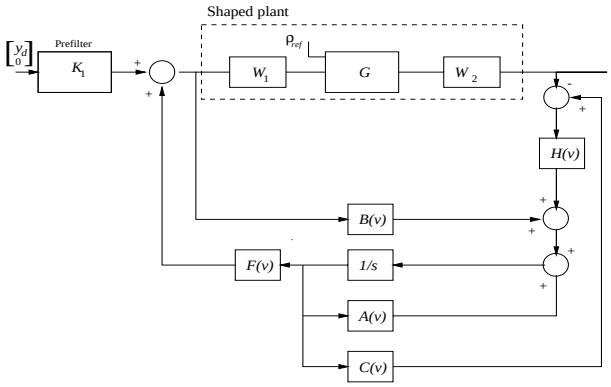

Fig. 20. Observer structure implementation.

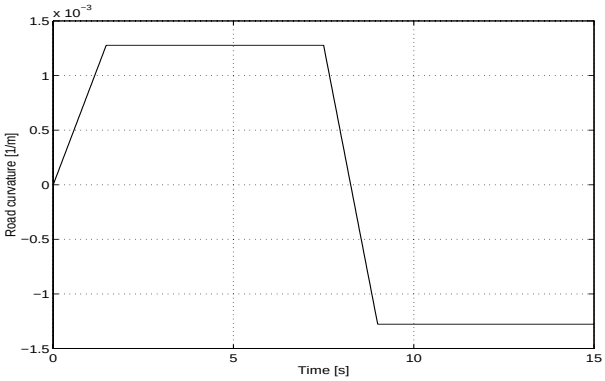

Fig. 21. Road curvature profile.

v	20	25	30	35	40
ϵ_{max}	0.561	0.548	0.539	0.532	0.527
k_1	1.485	1.575	1.646	1.704	1.753
k_2	1.414	1.444	1.468	1.487	1.504

Table 1. Optimized values for speed grid.

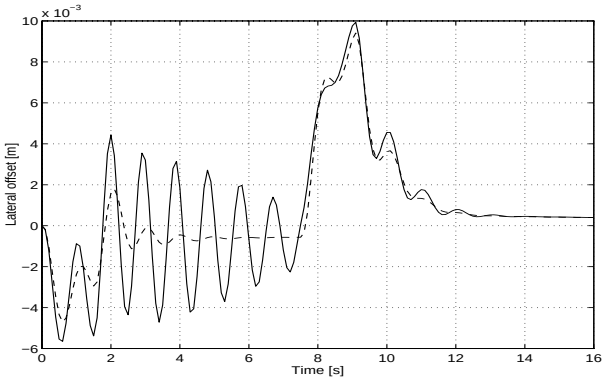

Fig. 22. Lateral offset, fixed and scheduled controller.

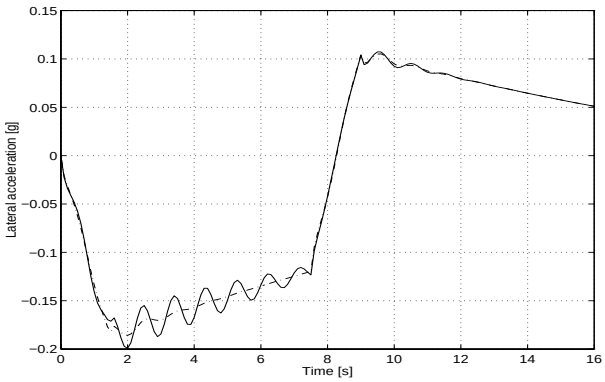

Fig. 23. Lateral acceleration, fixed and scheduled controller.

7. CONCLUSIONS

In this paper, the two-degree-of-freedom H_∞ optimization applied to automatic vehicle steering has been presented. The synthesis methodology simply allows direct specification of the time domain objectives. The whole synthesis procedure is emphasized and the obtained controller is tested on several typical automated highway maneuvers. The speed scheduling of the controller is then considered. The approach is found to be able to improve ride quality, the responses of the system are less oscillatory. However all the maneuvers are accomplished within system constraints and imposed limits of safety and comfort. In comparison with other control methods such as sliding mode [1], only the road relative lateral displacement and yaw angle are needed to be measured. These variables may be provided by a single sensor such as a video camera.

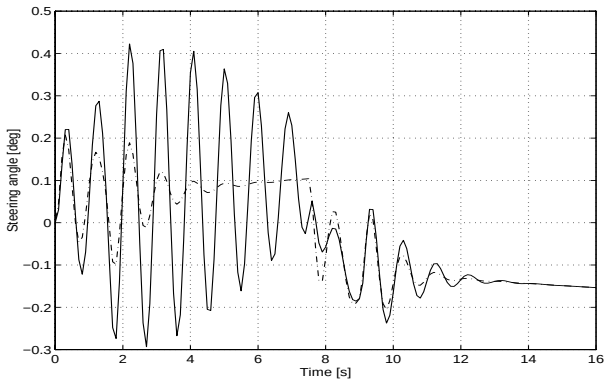

Fig. 24. Steering angle, fixed and scheduled controller.

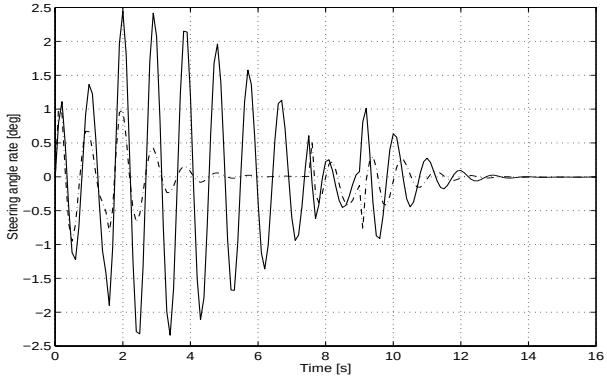

Fig. 25. Steering angle rate, fixed and scheduled controller.

REFERENCES

1. Ackermann, J., Guldner, J., Sienel, W., Steinhauser, R. and Utkin, V.I.: Linear and nonlinear controller design for robust automatic steering. IEEE Transactions on Control Systems Technology, Special Issue on Automotive Control 3 (1995), pp.132-143.
2. Doyle, J.C., Glover, K., Khargonekar, P. and Francis, B.: State-space solutions to standard H_2 H_∞ control problems. IEEE Transactions on Automatic Control 34 (1989), pp.831-848.
3. Gahinet, P., Nemirovski, A., Laub, A.J. and Chilali, M.: LMI Control Toolbox. The MathWorks, 1995.
4. Limebeer, D.J.N., Kasenally, E.M. and Perkins, D.: On the Design of Robust Two Degree of Freedom Controllers. Automatica 29(1) (1993), pp.157-168.
5. Mammar, S. and Duc, G.: Loop shaping H_∞ design: Application to the robust stabilization of a helicopter. Control Eng. Practice 1(2) (1993), pp.349-356.
6. Mammar, S.: H_∞ Robust Automatic Steering of a Vehicle. Proceedings of 1996 IEEE Intelligent Vehicles Symposium, Tokyo, 1996, pp.19-24.
7. Mammar, S.: Electrical Car Robust Lateral Control. 4^{th} World Congress on Intelligent Transportation Systems, Berlin, 1997.
8. Mammar, S.: Robust Reduced Order H_∞ Control for Tractor-Semitrailer Lateral Control. Proc. American Control Conference, San Diego, CA, USA, 1999, pp.3158-3162.

9. McFarlane, D. and Glover, K.: A loop Shaping design procedure using H_∞ synthesis. IEEE Transactions on Automatic Control 37 (1992), pp.759-769.
10. McFarlane, D. and Glover, K.: Robust Controller Design using Normalized Coprime Factor Plant Descriptions. Lecture Notes in Control and Information Science. Springer Verlag, Berlin, 1990.
11. O'Brien, R.T., Iglesias, P.A. and Urban, T.J.: Lane Change Maneuver via H_∞ steering Control. 4th IEEE Conference on Control Applications, Albany, 1995.
12. O'Brien, R.T., Iglesias, P.A. and Urban, T.J.: Vehicle lateral control for automated highway systems. IEEE Transactions on Control Systems Technology 4(3) (1996), pp.266-273.
13. Pham, H., Hedrick, K. and Tomizuka, M.: Combined Lateral and Longitudinal Control of Vehicles. Proc. American Control Conference, Baltimore, USA, 1994, pp.1205-1206.
14. Peng, H. and Tomizuka, M.: Vehicle Lateral Control for Highway Automation. Proc. American Control Conference, San Diego, CA, USA, 1990, pp.788-794.
15. Vinnicombe, G.: Frequency Domain Uncertainty and the Graph Topology. IEEE Transactions on Automatic Control 38 (1993), pp.1371-1383.
16. Hyde, R.A.: The Application of Robust Control to VSTOL Aircraft. PHD Dissertation, Girton College, Cambridge, 1991.
17. Walker, D.J. and Postlethwaite, I.: Advanced Helicopter Flight Control Using Two-Degree-of-Freedom H_∞ Optimization. Journal of Guidance, Control and Dynamics 19(2) (1996), pp.461-468.
18. Stilwell, D.J. and Rugh, W.J.: Interpolation of Observer State Feedback Controllers for Gain Scheduling. IEEE Transactions on Automatic Control 44 (1999), pp.1225-1229.